Pak. J. Bot., 55(6): 2179-2186, 2023. DOI: http://dx.doi.org/10.30848/PJB2023-6(10)

COMPARATIVE ANTIMICROBIAL ANALYSIS OF GREEN SYNTHESIZED SILVER NANOPARTICLES USING *BERBERIS LYCIUM* ROOT EXTRACTS AND BERBERINE

ASIA NOUREEN, FARHAN YOUNAS, IKRAM ULLAH AND MASOOM YASINZAI*

Centre for Interdisciplinary Research in Basic Sciences, International Islamic University, Islamabad, Pakistan 44000
**Corresponding author's email: masoomyasinzai588@gmail.com*

Abstract

Due to their significant biological potential, nanoparticles have been a focus of recent research. For the synthesis of the silver nanoparticles, pure berberine and aqueous root extracts of *Berberis lycium* were employed. Analytical methods like UV-Visible spectroscopy, FT-IR, SEM, and XRD were used to characterize the nanoparticles' structural and functional properties. The particles were spherical in shape with an average crystal size of Berberine AgNPs 47nm and of *B. lycium* root extract AgNPs was 16nm. MIC of *B. lycium* root extract AgNps was 1.5µg/ml with IC_{50} of 2.463 and MIC of berberine AgNps was 2.5µg/ml and IC50 of 2.599 against *E. coli*. MIC of *B. lycium* root extract AgNps was 1.5µg/ml and IC50 of 2. 514 and MIC of berberine AgNps was 1.5µg/ml and IC50 of 2.922 against *S. aureus*. The nanoparticles synthesized with root extracts were found to be more potent as antibacterial agents.

Key words: *Berberis lycium*, Berberine, Green synthesis, Nanoparticles, Antimicrobials.

Introduction

The nanotechnology is a reliable environment friendly procedure for the development of nano scale particles ranging from 1-100 nm (Ramya & Subapriya, 2012). Biosynthesis is preferred, as high temperature and dangerous chemicals are not required (Fedlheim & Foss, 2001; Forough & Fahadi, 2011). Due to their important electrical, synergistic, and photodynamic properties, metal nanoparticles have been a focus of ongoing research. Massive efforts have been made to regulate and improve the size and shape of nanoparticles because these factors are crucial to adjusting their optical, chemical, and physical properties, respectively (Alivisatos, 1996; Bruchez Jr, 1998; Coe *et al*., 2002).

B. lycium Royle is considered as a medicinal plant and different species of this plant are used worldwide. The root and bark extract is being used to treat various diseases including urinary tract infection, spleen, liver disorders, and gastric and duodenal ulcers (Chauhan *et al*., 2009; Chiang *et al*., 1977). This plant has been previously reported to contain various types of secondary metabolites such as steroids and alkaloids. Most of the biologically significant, active, and isolated chemical compounds are berberine and palmatine (Kinghorn & Poshusta, 1993). Berberine and its correspondent derivatives show an organic class of cations, that is derived from various generic plants of Berberis, Mohania, and Coptis. These chemicals have represented broad applications for anticarcinogenic, antimicrobial, and antimutagenic activities, respectively (Chiang *et al*., 1977; Chopra, 1958). According to (Bhardwaj & Kaushik, 2012) The primary active component in almost all Berberis species has been identified as berberine. Berberine is the most abundant phytochemical in *B. lycium* root. 4.0% berberine in *B. lycium* roots and 2.8% berberine in stem bark has been reported earlier (Andola *et al*., 2010). The *B. lycium* species is highly significant biologically and is also used as a household medicine in Pakistan. Green nanotechnology is an eco-friendly technology. It tunes and governs the nanotechnology's principles by controlling the matter and shape of the world that varies from 'atom by atom' into a green environment (Iravani, 2011). Therefore, we come across a new green nano world in which the process of production is optimized, and based on the waste-free method. Hazardous wastes getting to the environment cannot be easily identified and decomposed (Schwarz, 2009). Comprehensively, it is well documented that silver-based nanoparticles and silver ions are hazardous to all microorganisms including 16 bacterial species (Mendil & Uluözlü, 2007). When manufactured silver nanoparticles are employed, the increased surface area make the microbes more susceptible. Silver (Ag) is used in the form of nitrate to boost the antibacterial effect. Although, AgNPs have a tremendous role in various antibacterial applications, however, the interaction of the silver metal with microbes is not fully understood yet.

AgNPs are thought to cause cellular inhibition, transduction and lysis. Furthermore, several mechanisms have been reported that are involved in cell growth inhibition and cell lysis (Prabhu & Poulose, 2012). Being a mild acid in chemistry, silver is predisposed to interacting with bases. Cells are mostly made up of phosphorus and sulfur which are soft bases in nature. Due to this mechanism of action nanoparticles treatment leads to apoptosis. Interestingly, it may also be of importance that the DNA molecule is made up of phosphorus and sulfur backbone, consequently, the DNA molecule can be destroyed by the AgNPs intense intercalation of these bases, leading to cell death. (Morones *et al*., 2005). When AgNPs intercalates DNA's phosphorus and sulphur backbone, they cause a variety of issues that ultimately stop all DNA replication in bacteria. (Hatchett & White, 1996). This work intends to investigate the comparative analysis of antibacterial potential of green synthesized AgNPs of *B. lycium* root extract and AgNPs of berberine.

Materials and Methods

Collection of plant and extraction: Roots of the *B. lycium* plant were harvested in Murree, Pakistan, twice rinsed, shade dried and milled. Berberine was purchased as a chloride salt from Sigma Aldrich USA (CAS No 633-65-8). After being heated (60°C/ 30 mints), the root extract and Berberine (5 g each) were

weighed into 50 ml of de-ioinized water. The mixture was incubated under shaking at RT/48 hrs and filtered through whatman filter paper (90mm pore size).

Green synthesis of AgNPs: The extract was mixed and incubated the desired concentration of Silver nitrate (Aldrich 209139; silver nitrate 99.9%) at the ratio of 1:2 for 24 hrs. The salt was used in six different concentrations (ImM, 2.5mM, 5mM, 7.5mM, l0mM, and l5mM). Visible change in color suggested the successful reduction of Ag. The solution was then centrifuged at 10,000 rpm/10 mins (Bagheri *et al*., 2016). These AgNPs were dried under room conditions.

Optimization of parameters for the synthesis of silver nanoparticles: Salt concentration, pH, temperature and incubation period were some of the factors which were assessed at varying concentrations to have the best yield and morphological features of the NPs.

Concentrations of plant extracts, silver nitrate solution: A series of plant extracts and salt concentrations were tested to find out the optimum concentrations. Plant extract was tested at 0.25, 1.25, 2.5, and 7.5 mg/ml, and salt solution at (1mM, 2.5mM, 7.5mM, 10mM, 15mM). The reaction mixtures were incubated in the dark under room conditions.

Conditions optimization: pH for the synthesis protocol was optimized using the already available protocol (Mittal *et al*., 2012). pH range of 2.0-9.0 was tested. pH adjustment was done either by adding 0.1M NaOH or 0.1M HCl. AgNPs were synthesized at different temperature (25°C, 35°C, 45°C and 60°C) in a static incubator (JSSI-300CL, Korea). The reaction mixtures were kept in dark conditions. Due to the significance of incubation time synthesis of AgNPs was assessed at different reaction times (30 minutes, 1hr, 2hrs, 3hrs, 4hrs and 24hrs). The reaction mixtures were kept in the dark while keeping other parameter constant.

Characterization of silver nanoparticle

UV-visible spectroscopy: UV-visible spectrophotometer (PerkinElmer Lambda 950UV/Vis's spectrophotometer, UK) was used to detect the successful bio-reduction of silver ions between 200nm-700nm wavelengths at a resolution of 1nm.

Fourier transform infrared spectroscopy (FTIR): FT-IR (Perkin-Elmer spectrum 100, United States) was used for the functional groups identification. Spectra of both the synthesized silver NPs were recorded at the range of 1000 and 4000 cm^{-1}.

X-Ray diffraction (XRD) analysis: Phase purity, grain size and crystallinity of AgNPs was determined by XRD (Rigaku Geiger Flex D-max III/c diffractometer, USA). The lypholized samples were analyzed on silica supports. The analysis were performed at the range of 2° from 30 to 70° by a copper ray tube operated at 30 Kv and 20mA.

Scanning electron microscopy (SEM): SEM (JSM 6390LV, JOEL, USA) was utilized for the morphological characterization of the synthesized particles.

Antibacterial activity: 0.5 McFarland standards ($1x10^8$ CFU/ml) of fresh culture of bacteria were inoculated after 24hours of incubation on Muller Hinton Agar plate. Different concentrations of AgNPs of *B. lycium* and AgNps of Berberine (1.5, 3, 6.25, 12.5, 25, 50, 100 µg/ml) were serially dispensed in the wells. Positive control (0.05% Pen-strep) and negative control (H_20) were used. Zones of inhibition (ZOI) in mm were measured post 24 hrs incubation at 37°C.

MIC values were calculated using an already established protocol (Mehmood *et al*., 2016). AgNPs were used at a final concentration of. Each well contained 10 µL of 100µg/ml nanoparticles, 10 µL of the inoculum and 180 µL nutrient broth medium. OD_{620} was measured post 24 hrs incubation at 37°C.

Results

Green synthesis of silver nanoparticles: Color change was observed from yellowish to dark brown when *B. lycium* root extract mixed with silver nitrate salt solution which was the initial indication of silver nanoparticles formation.

Concentrations of plant extracts, silver nitrate solution: Different concentrations of the plant extract (0.25, 1.25, 2.5, 5 and 7.5 µg/ml) were used. Silver nitrate was utilized at concentration ranging from 0.25 to 15mM, and the optimal value of silver nitrate salt solution concentration was 10mM. The yield of AgNPs increased with the increasing concentration of $AgNO_3$. (Park *et al*., 2012).

Conditions optimization: At different pH values AgNPs synthesis was optimized but neutral pH was optimal i-e pH-7. In terms of reaction temperature, the method of AgNPs biological synthesis has the advantage of producing stable nanoparticles at room temperature (25°C). After assessing the synthesis at a range of temperature points, room temperature (25°C) was found to be the optimal temperature because at room temperature small and spherical AgNPs were synthesized and showed single plasmon resonance at UV-visible spectroscopy. AgNPs were synthesized at all reaction times but the yield was different at different reaction times. The yield of AgNPs increased with the increasing Ag concentration and time (Mashwani *et al*., 2015). 12 hrs incubation period in the dark resulted in better yield of AgNPs with a single and short wavelength peak at UV-visible spectroscopy.

UV-visible spectroscopy: As a result of AgNPs' activation of surface plasmon resonance (SPR), the colloidal solution's color altered. Due to excitation of (SPR) UV-spectrum of the biosynthesized silver nanoparticles of *B. lycium* root extract (Fig. 1) (a) and berberine Figure 1 (b) showed absorbance at 400 nm and 432 nm respectively.

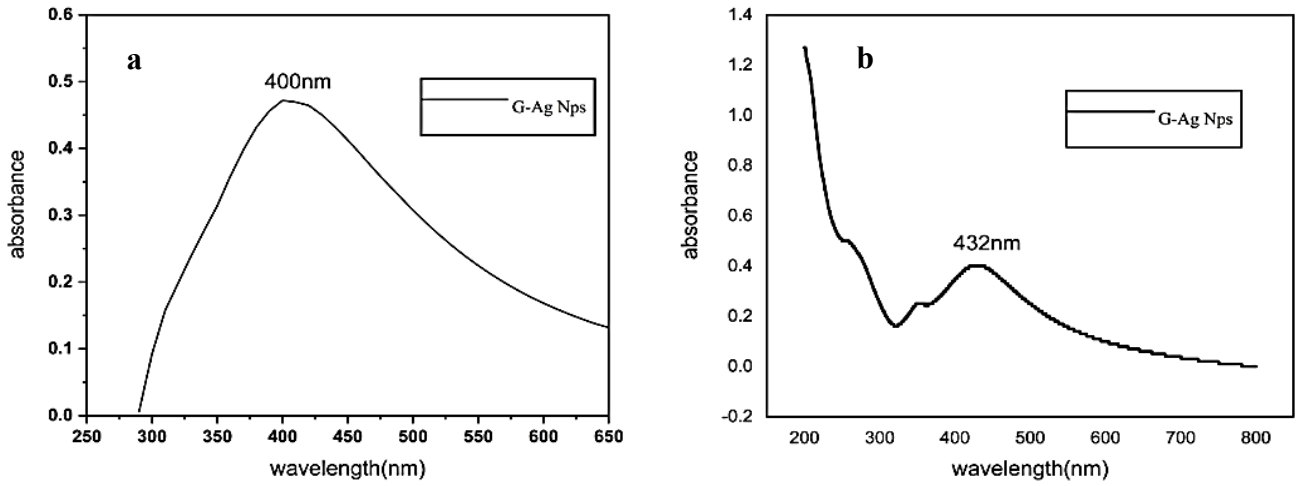

Fig. 1. UV-vis absorption spectrum of silver nanoparticles. Fig. 1(a) AgNPs of *Berberis lycium* root extract Fig. 1(b) AgNPs of Berberine.

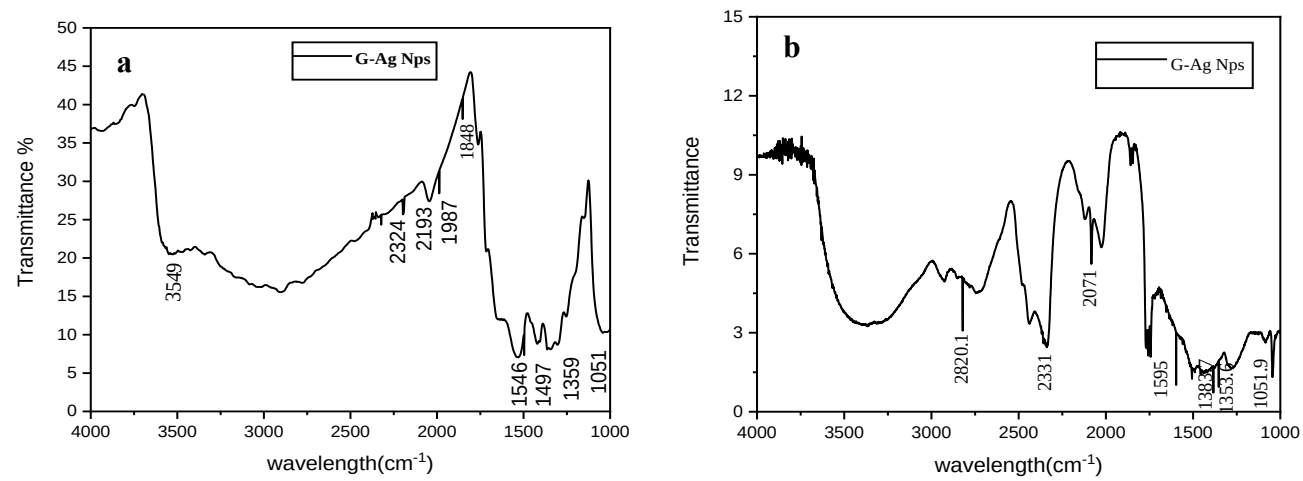

Fig. 2. FT-IR spectrum of synthesized Ag NPs of *Berberis lycium* root extract Fig. 2(a) and FT-IR spectrum of Ag nanoparticles of Berberine Fig. 2(b).

Fourier transform infrared spectroscopy (FT-IR): The bands at 3549, 2324, 2193, 1987, 1848, 1546, 1497, 1359 and 1051cm $^{-1}$ were observed in FT-IR spectrum for *B. lycium* RE (Fig. 2) (a). The spectrum at 3549 cm^{-1} were assigned for OH stretching of alcohol. 2324cm^{-1} was attributed to C-H stretching of aldehyde. 2193cm^{-1} were assigned for carbon triple bond of alkynes. 1987cm^{-1} for C=C asymmetric stretch.1848cm^{-1} for C=O stretching of aldehyde. The peak at 1546 cm^{-1} was strong C-N stretching. 1497cm^{-1} were assigned for C-C stretching or C-N of aromatic amine group or C=C of aromatic ring. The peak at 1359 cm^{-1} was strong C-N stretching of aromatic compounds and the peak at 1051 cm^{-1} was assigned for C-O starching. Figure 2 (b) shows the bands at 2820.1, 2331, 2071, 1595, 1383.7, 1353.6, and 1051.9cm^{-1} of berberine. The peak at 2820.1cm^{-1} was assigned for -C-H stretching. The peak at 2331cm^{-1} were assigned for C-H stretching of aldehyde. The peak at 2071cm^{-1} were assigned for C≡C.1595cm^{-1} were assigned for C=C and C=N stretching.1353-1383 cm^{-1} were specified for C-H stretching. 1051 cm^{-1} were specified for C-O stretching.

X-Ray diffraction analysis: The diffraction peaks of both AgNPs were observed in the 2Θ range of 30–70°, which could be attributed to (101) (102) (110) for *B. lycium* (Fig. 3 (a) and (111) (200) (220) for berberine AgNPs (Fig. 3) (b) . Consequently, it was confirmed that both the nanoparticles have crystalline cubic (CC) structure. In both cases, the results are in accordance with the international pattern of joint committee on powder diffraction data (JCPDS NO. 00-003-0921) (Jung *et al*., 1926). The crystallinity of the synthesized nanoparticles was confirmed by the intensity of the peaks, however, as indicated by the broad diffraction peaks, they are most probably small crystallites. (I.A. Wani *et al*., 2011). Peaks intensity, position and width, full width at half-maximum (FWHM) were calculated from the XRD pattern. The average particle size was calculated using Debye-Scherrer equation (Bykkam *et al*., 2015).

$$D=k\lambda / \beta\cos\Theta$$

where K being Scherrer's having the assigned value of 0.94, λ is the radiation wavelength (1.5406 A); β is the

value of FWHM (radians), Θ = diffraction angle (Dubey *et al*., 2010).

The FWHM of the *B. lycium* AgNPs most isolated peaks at about 38° (101), 44 (102) and 64° (110) in 2 Θ were used for size evaluation. The average crystallite size was determined to be 16nm. The FWMH of the berberine AgNPs most isolated peaks at about 38° (111), 44° (200), and 64° (220). For berberine the average crystal size was 47nm.

Scanning electron microscopy (SEM): The synthesized particles were found to be spherical and having average diameter below 100 nm. SEM images of AgNPs of *B. lycium* (Fig. 4) (a) show spherical shape. The average size of the AgNPs of *B. lycium* was found in the range of 47nm. SEM images of AgNPs of Berberine (Fig. 4) (b) powder is observed and found that the particles are in nano-size. The diameter of AgNPs were below 100nm and the average size was found in the range of 65-66nm.

Antibacterial activity: Based on the results of antimicrobial activity, the particles were found to be significantly potent against *E. coli* and *S. aureus*. Varying zones of inhibition were observed at (0.75, 1.5, 3, 6.25, 12.5, 25, 50 and 100µg/ml). Negative control (H_2O) and positive control (pen-strip) were used. Silver nanoparticles of *B. lycium* root extract (Fig. 5) (a) showed highest activity against *E. coli (*14.66±0.57mm) at 100µg/ml. The particles were found to be not highly potent against *E. coli* (9 ±1mm). The zone of inhibition of negative control (0±0mm) and positive control (22±0mm). The AgNPs of *B. lycium* root extract at concentration (6.2, 3, 1.5 and 0.75µg/ml) did not show any activity. Minimum inhibitory concentration (MIC) of AgNPs *B. lycium* root extract (Fig. 6) (a) was 1.5µg/ml and IC50 value 2.463.

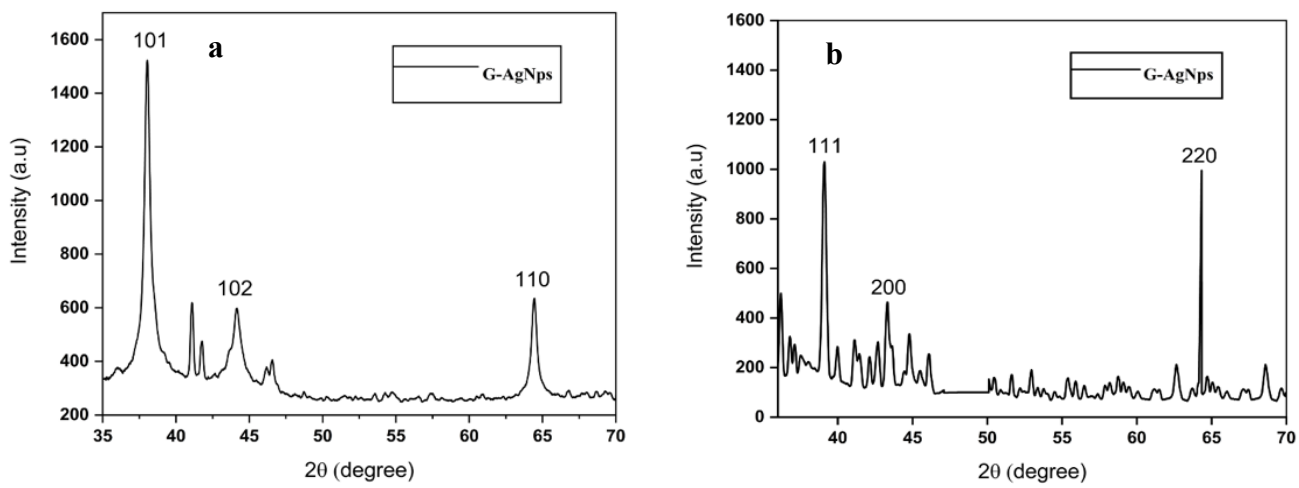

Fig. 3. XRD pattern of Ag NPs of *B. lycium* root extract Fig. 3(a) and XRD pattern of AgNPs of berberine Fig. 3(b).

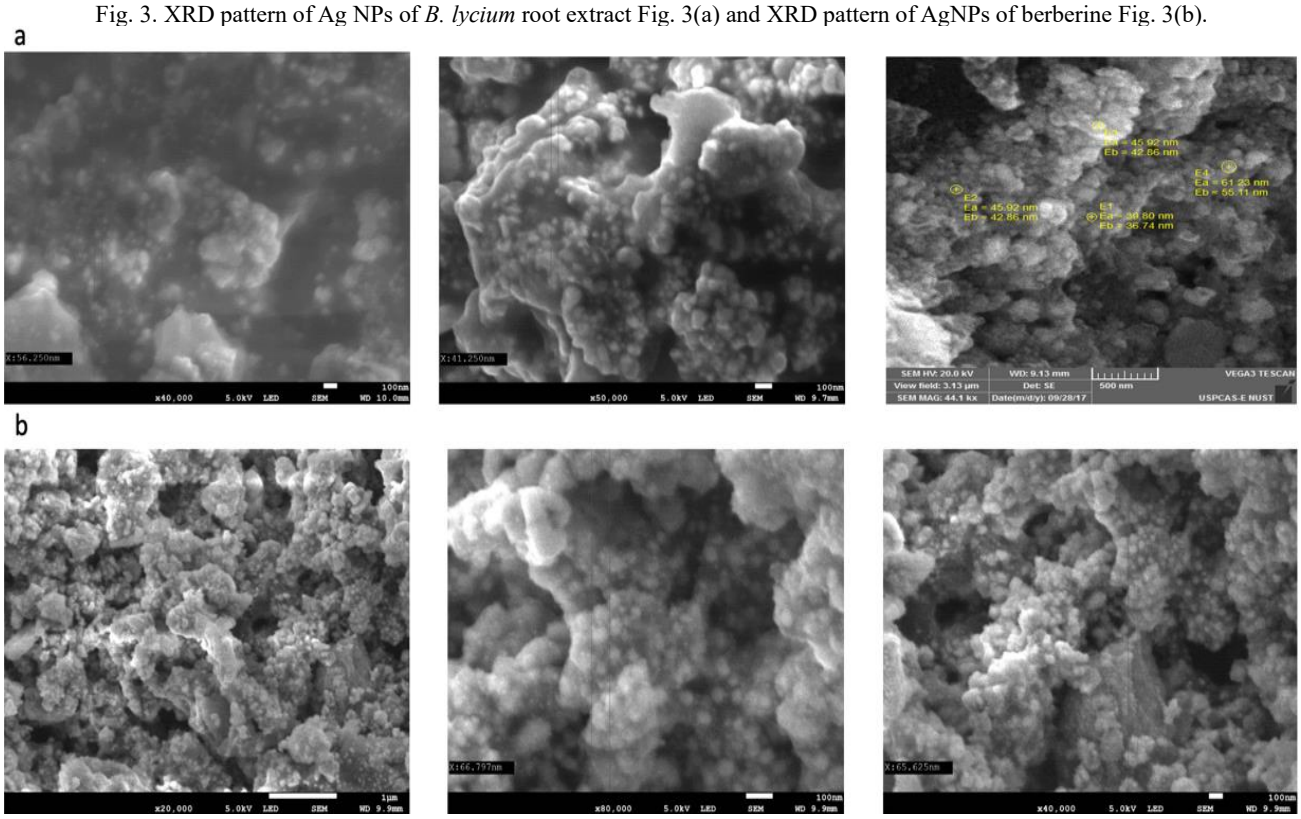

Fig. 4. SEM images of synthesized AgNPs of *B. lycium* root extract Fig. 4(a) and SEM images of AgNPs of berberine Fig. 4(b).

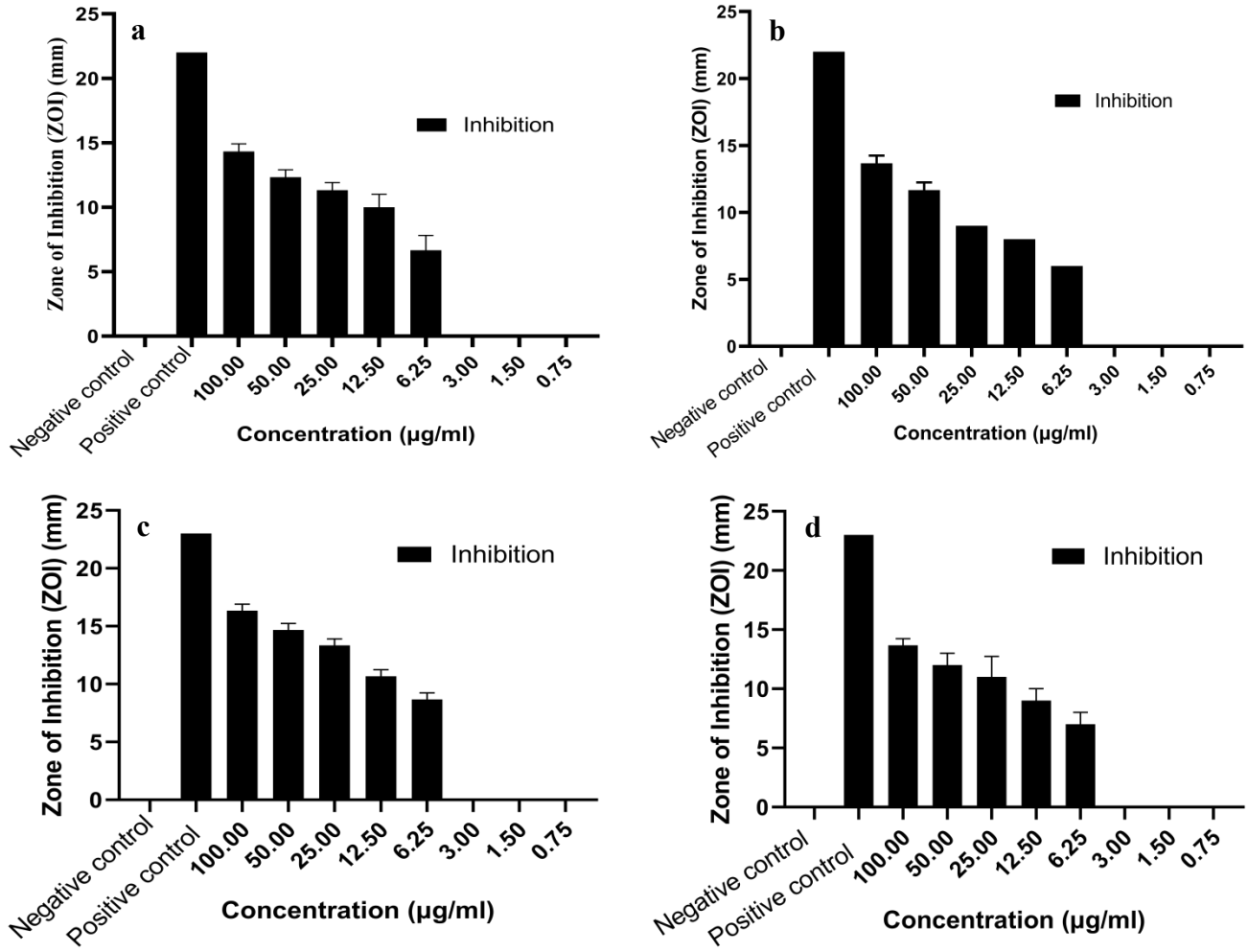

Fig. 5. Graphical presentation of Antibacterial activity of AgNPsof *B. lycium* root extract Fig. 5(a) and AgNPs berberine Fig. 5(b) by agar well diffusion method against *E. coli*.
Antibacterial activity of AgNps of *B. lycium* root extract Fig. 5(c) AgNps of *B. lycium* root extract and AgNps berberine Fig. 5(d) by agar well diffusion method against *S. aureus*.

The AgNPs of *B. lycium* root extract Fig. 5 (c) showed highest activity against *S. aureus* (16.33±0.57mm) at 100µg/ml. The lowest activity was reported against *S. aureus* (8.66±0.57mm). The zone of inhibition of negative control H2O (0±0mm) and positive control pen strip (23±0mm). Minimum inhibitory concentration (MIC) of AgNps *B. lycium* root extract Fig. 6 (c) was 1.5µg/ml and IC50 value 2. 514. The AgNPs of *B. lycium* root extract at concentration (3, 1.5 and 0.75µg/ml) did not show any activity.

In comparison the biologically synthesized AgNPs of berberine Fig. 5 (b) showed highest activity against *E. coli* (13.66±0.57mm) at 100µg/ml. The lowest antibacterial activity of AgNPs berberine was reported against *E. coli* (6±0mm). At concentration of (3, 1.5 and 0.75µg/ml) AgNPs of berberine did not show any activity. Minimum inhibitory concentration (MIC) of AgNPs berberine Fig. 6 (b) was 2.5µg/ml and IC50 value 2.599.

The AgNPs of berberine showed (Fig.5 (d) highest activity against *S. aureus* (13.66±0.57mm) at 100µg/ml. The lowest antibacterial activity of AgNps berberine was reported against *S. aureus* (7±1mm). At concentration of (3, 1.5 and 0.75µg/ml) AgNPs of berberine did not show any activity. Minimum inhibitory concentration (MIC) of AgNps berberine Fig. 6 (d) was 1.5µg/ml and IC50 value 2.922.

Discussion

Colour change to brown in the reaction mixture due to surface plasmon resonance is an indication of the successful synthesis of AgNPs (Hyllested *et al*., 2015; Lalitha *et al*., 2013). Several factors i.e. concentration of plant extract and salt, pH, Temperature and time are crucially important in the synthesis of AgNPs (Ahmed *et al*., 2016; Krishnaraj *et al*., 2010). The optimum conditions are reported to be neutral pH, RT and an incubation period of 12 hrs (Banerjee *et al*., 2014; Vigneshwaran *et al*., 2006). The reduction of $AgNO_3$ to Ag+ ions in the aqueous solution is confirmed the UV-Vis spectrum. Many studies have reported the SPR for colloidal silver ranging from 320-390nm (Huang & Yang, 2004) while others reported 420-450nm (Banerjee *et al*., 2014) 400-500nm (Mehmood *et al*., 2014).

Proteins and other bioactive substances stabilised the AgNPs surface and stopped the electronic transition (Otunola *et al*., 2017). The data showed the presence of only AgNPs in the dispersion.

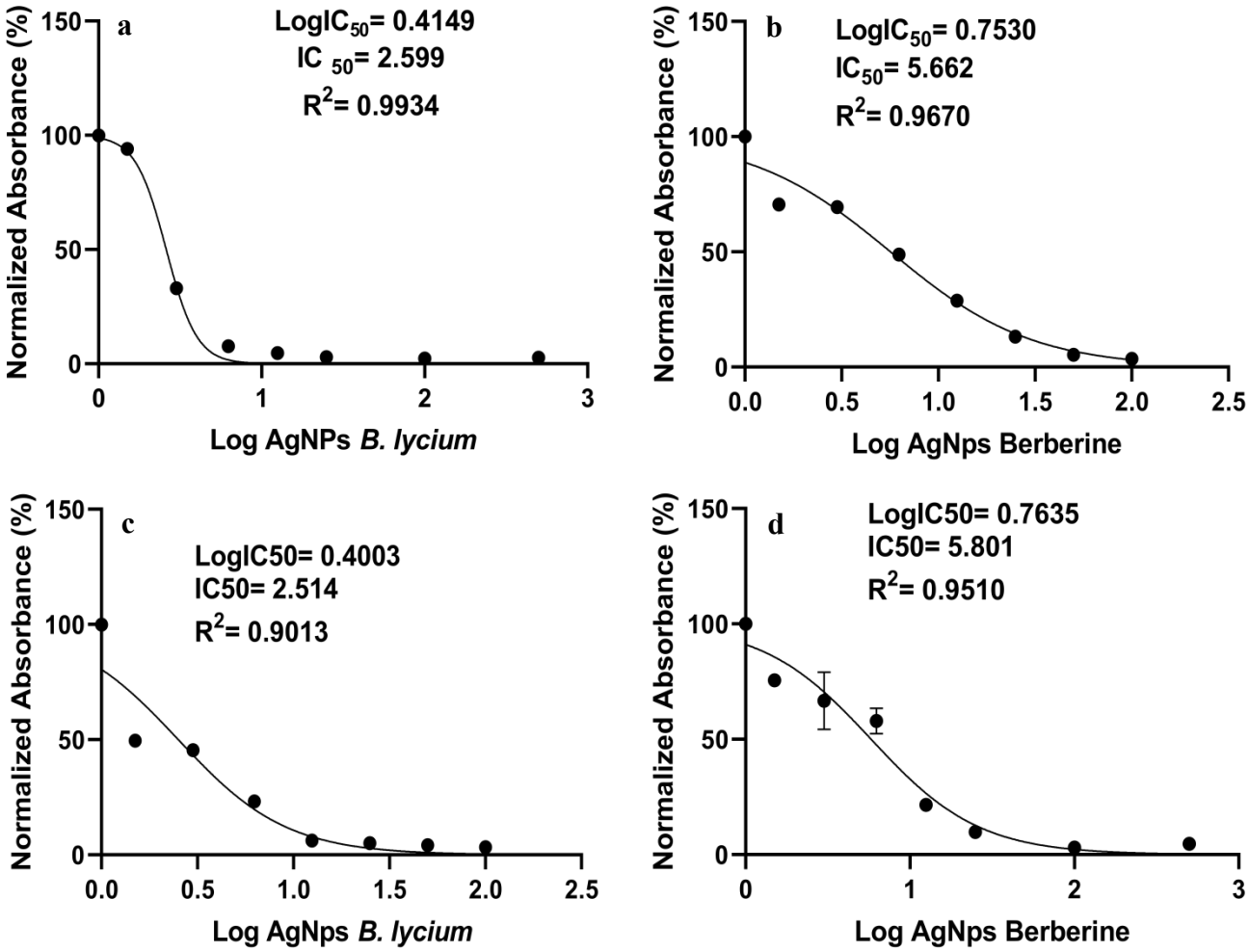

Fig. 6. Minimum inhibitory concentration of AgNPs of *B. lycium* root extract and Berberine against *E. coli*. MIC of AgNPs *B. lycium* root extract Fig. 6(a) and MIC of AgNPs of Berberine Fig. 6(b). MIC of AgNPs*B. lycium* root extract Fig. 6(c) and berberine Fig. 6(d) against *S. aureus*.

FT-IR spectrum of a pure compound can literally serve as a molecular fingerprint (Sasidharan *et al*., 2011). It has been observed that a range of compounds in the extracts i.e phenols, flavonoids, terpenoids and proteins might be serving as stabilizers and capping agents in the AgNPs synthesis (Mehmood *et al*., 2016). Several studies on AgNPs from plant extracts of *Urtica dioica* have been reported (Jyoti *et al*., 2016), *Lippia nodiflora* (Liu *et al*., 2007), *Azadirachta indica* (Ahmed *et al*., 2016) and *Pedalium murex* (Khanna & Nair, 2009). XRD pattern indicated that the peaks were readily of silver as reported previously as well (Mubayi *et al*., 2012).

SEM is intensively utilized to study the topography and morphology of a particle. In accordance to the previous reports, our AgNPs also had spherical as well as rectangular shape and had high density (Theivasanthi & Alagar, 2011). Enhanced surface area of the synthesized particles make them more biologically potent. The different size of the NPs may be due to different compounds in the extract which can have a role in the capping.

It is known from the literature that Silver nanoparticles are lethal to all microorganisms and cause cell growth inhibition and cell lysis (Prabhu & Poulose, 2012). Some of the mechanism which contribute to the biological potential of the silver nanoparticles include: enhanced membrane permeability and cellular accumulation, however, the mode of action needs to be further investigated (Sondi & Salopek-Sondi, 2004).

Conclusion

Using biomaterial for the synthesis of AgNPs is a cost effective and ecofriendly approach. Green synthesized AgNPs of *B. lycium* were more biological potent compared to Green synthesized AgNPs of Berberine which shows that, In *B. lycium* root extract different compounds are present with Berberine which have might some synergistic effects to enhance the antibacterial activity. Berberine was discovered to be 80 percent dry weight in the root extract of *B. lycium*, with only traces of other alkaloids present. In comparison the antibacterial activity of Green synthesized AgNPs of pure compound Berberine was positive but less than AgNPs of

B. lycium root extract. The characterization results suggest that berberine may be the key compound involved in the synthesis of AgNPs. This kind of approach is needed to tackle multidrug resistance microbes.

Acknowledgments

The authors would like to sincerely pay gratitude to Late Prof. Dr. Abdul Hameed in the initiation and execution of the project.

References

Ahmed, S., Saifullah, M. Ahmad, B.L. Swami and S. Ikram. 2016. Green synthesis of silver nanoparticles using Azadirachta indica aqueous leaf extract. *J. Radiat Res. Appl. Sci*., 9: 1-7.

Alivisatos, A.P. 1996. Semiconductor clusters, nanocrystals, and quantum dots. *Science*, 271: 933-937.

Andola, H., R. Rawal, M. Rawat, I. Bhatt and V. Purohit. 2010. Analysis of berberine content using HPTLC fingerprinting of root and bark of three Himalayan Berberis species. *Asian J. Biotechnol*., 2: 239-245.

Bagheri, A., H. Arandiyan, C. Boyer and M. Lim. 2016. Lanthanide-doped upconversion nanoparticles: emerging intelligent light-activated drug delivery systems. *Adv. Sci*., 3: 150-437.

Banerjee, P., M. Satapathy, A. Mukhopahayay and P. Das. 2014. Leaf extract mediated green synthesis of silver nanoparticles from widely available Indian plants: synthesis, characterization, antimicrobial property and toxicity analysis. *Biores. Bioproc*., 1: 1-10.

Bhardwaj, D. and N. Kaushik. 2012. Phytochemical and pharmacological studies in genus Berberis. *Phytochem. Rev.,* 11: 523-542.

Bruchez, Jr. M.P. 1998. Luminescent semiconductor nanocrystals: Intermittent behavior and use as fluorescent biological probes. University of California, Berkeley.

Chauhan, N., D. Kumar and M. Kasana. 2009. Medicinal plants of Muzaffarnagar district used in treatment of urinary tract and kidney stones. *Ind. J. Trad Knowl*., 8: 191-195.

Chiang, M., B. Chiang and W. Grant. 1977. Transfer of resistance to race 2 of Plasmodiophora brassicae from *Brassica napus* to cabbage (*B. oleracea* var. *capitata*). I. Interspecific hybridization between *B. napus* and *B. oleracea* var. *capitata*. *Euphytica*., 26: 319-336.

Chopra, H.C. 1958. Morphological and histochemical study of oocytes of the fish, Barbus ticto (Punctius), with particular reference to lipids. In: *Research Bull. Pad! jab Univ*.

Coe, S., W.K. Woo. M. Bawendi and V. Bulović. 2002. Electroluminescence from single monolayers of nanocrystals in molecular organic devices. *Nature*, 420: 800-803.

Dubey, S.P., M. Lahtinen and M. Sillanpää. 2010. Tansy fruit mediated greener synthesis of silver and gold nanoparticles. *Process Biochem*., 45: 1065-1071.

Fedlheim, D.L. and C.A. Foss. 2001. Metal nanoparticles: synthesis, characterization, and applications. CRC press.

Forough, M. and K. Fahadi. 2011. Biological and green synthesis of silver nanoparticles. *Turk. J. Eng. Environ. Sci*., 34: 281-287.

Hatchett, D.W. and H.S. White. 1996. Electrochemistry of sulfur adlayers on the low-index faces of silver. *The J. Physical Chem*., 100: 9854-9859.

Huang, H. and X. Yang. 2004. Synthesis of polysaccharide-stabilized gold and silver nanoparticles: a green method. *Carbohyd. Res*., 339: 2627-2631.

Hyllested, J.A.E., M.E. Palanco, N. Hagen. K.B. Mogensen and K. Kneipp. 2015. Green preparation and spectroscopic characterization of plasmonic silver nanoparticles using fruits as reducing agents. *Beilstein J. Nanotech*., 6: 293-299.

Iravani, S. 2011. Green synthesis of metal nanoparticles using plants. *Green Chem*., 13: 2638-2650.

Iravani, S. and B. Zolfaghari. 2013. Green synthesis of silver nanoparticles using Pinus eldarica bark extract. *Biomed Res Int*.,

Jyoti, K., M. Baunthiyal and A. Singh. 2016. Characterization of silver nanoparticles synthesized using *Urtica dioica* Linn. leaves and their synergistic effects with antibiotics. *J. Radiat Res. Appl. Sci*., 9: 217-227.

Khanna, P.K. and C. Nair. 2009. Synthesis of silver nanoparticles using cod liver oil (fish oil): green approach to nanotechnology. *Int. J. Green Nanotechnol: Physics and Chemistry*, 1: P3-P9.

Kinghorn, D.B. and R. Poshusta. 1993. Nonadiabatic variational calculations on dipositronium using explicitly correlated Gaussian basis functions. *Phys. Rev. A*., 47: 3671.

Krishnaraj, C., E. Jagan. S. Rajasekar. P. Selvakumar. P. Kalaichelvan and N. Mohan. 2010. Synthesis of silver nanoparticles using *Acalypha indica* leaf extracts and its antibacterial activity against water borne pathogens. *Coll. Surf B. Biointerf*.,76: 50-56.

Lalitha, A., R. Subbaiya and P. Ponmurugan. 2013. Green synthesis of silver nanoparticles from leaf extract *Azhadirachta indica* and to study its anti-bacterial and antioxidant property. *Int. J. Curr. Microbiol. App. Sci*., 2: 228-235.

Liu, X., M. Atwater, J. Wang and Q. Huo. 2007. Extinction coefficient of gold nanoparticles with different sizes and different capping ligands. *Coll. Surf B. Biointerf*., 58: 3-7.

Mashwani, Z.U.R., T. Khan. M.A. Khan and A. Nadhman. 2015. Synthesis in plants and plant extracts of silver nanoparticles with potent antimicrobial properties: Current status and future prospects. *Appl. Microbiol. Biotechnol.*, 99: 9923-9934.

Mehmood, A., G. Murtaza, T.M. Bhatti, R. Kausar and M.J. Ahmed. 2016. Biosynthesis, characterization and antimicrobial action of silver nanoparticles from root bark extract of *Berberis lycium* Royle. *Pak. J. Pharm. Sci*., 29: 131-137.

Mehmood, A., G. Murtaza. T.M. Bhatti and R. Kausar. 2014. Enviro-friendly synthesis of silver nanoparticles using *Berberis lycium* leaf extract and their antibacterial efficacy. *Acta Metall. Sin.,* 27: 75-80.

Mendil, D. and Ö.D. Uluözlü. 2007. Determination of trace metal levels in sediment and five fish species from lakes in Tokat, Turkey. *Food Chem*., 101: 739-745.

Mittal, A.K., A. Kaler and U.C. Banerjee. 2012. Free radical scavenging and antioxidant activity of silver nanoparticles synthesized from flower extract of *Rhododendron dauricum*. *Nano. Biomed*. *Eng*., 4.

Morones, J.R., J.L. Elechiguerra. A. Camacho, K. Holt and J.B. Kouri, J.T. Ramírez and M.J. Yacaman. 2005. The bactericidal effect of silver nanoparticles. *Nanotech*., 16: 2346-2353.

Mubayi, A., S. Chatterji. P.M. Rai and G. Watal. 2012. Evidence based green synthesis of nanoparticles. *Adv. Mat. Lett.,* 3: 519-525.

Nadagouda, M.N. and R.S. Varma. 2008. Green synthesis of silver and palladium nanoparticles at room temperature

using coffee and tea extract. *Green Chem*., 10: 859-862.

Otunola, G.A., A.J. Afolayan. E.O. Ajayi and S.W. Odeyemi. 2017. Characterization, antibacterial and antioxidant properties of silver nanoparticles synthesized from aqueous extracts of *Allium sativum*, *Zingiber officinale*, and *Capsicum frutescens*. *Pharm. Mag*., 13: S201.

Park, Y., H.J. Noh. L. Han, H.S. Kim. Y.J. Kim. J.S. Choi, C.K. Kim, Y.S. Kim and S. Cho. 2012. *Artemisia capillaris* extracts as a green factory for the synthesis of silver nanoparticles with antibacterial activities. *J. Nanosci. Nanotechnol*., 12: 7087-7095.

Prabhu, S. and E.K. Poulose. 2012. Silver nanoparticles: Mechanism of antimicrobial action, synthesis, medical applications, and toxicity effects. *Int. Nano. Lett*., 2: 32.

Ramya, M. and M.S. Subapriya. 2012. Green synthesis of silver nanoparticles. *Int. J. Pharm. Med. Biol. Sci*., 1: 54-61.

Sasidharan, S., Y. Chen. D. Saravanan, K. Sundram and L.Y. Latha. 2011. Extraction, isolation and characterization of bioactive compounds from plants' extracts. *Afr. J. Trad. Comp. Altern. Med*., 8: 1-10.

Schwarz, A.E. 2009. Green dreams of reason. Green nanotechnology between visions of excess and control. *Nanoethics*., 3: 109-118.

Sondi, I. and B. Salopek Sondi. 2004. Silver nanoparticles as antimicrobial agent: a case study on E. coli as a model for Gram-negative bacteria. *J. Coll. Interf. Sci*., 275: 177-182.

Theivasanthi, T. and M. Alagar. 2011. Electrolytic synthesis and characterizations of silver nanopowder. arXiv preprint arXiv., 1111.0260.

Vigneshwaran, N., R. Nachane, R. Balasubramanya and P. Varadarajan. 2006. A novel one-pot 'green'synthesis of stable silver nanoparticles using soluble starch. *Carbohyd. Res*., 341: 2012-2018.

Zargar, M., A.A. Hamid. F.A. Bakar, M.N. Shamsudin, K. Shameli, F. Jahanshiri and F. Farahani. 2011. Green synthesis and antibacterial effect of silver nanoparticles using *Vitex negundo* L. *Molecules*, 16: 6667-6676.

(Received for publication 23 May 2022)